

Automated tracking for advanced satellite laser ranging systems

**Jan F. McGarry
John J. Degnan
NASA Goddard Space Flight Center
Greenbelt, Maryland**

**Paul Titterton
Harold Sweeney
The Electro-Optics Organization
Sunnyvale, California**

**Brion P. Conklin
AlliedSignal Technical Services
Columbia, Maryland**

**Peter J. Dunn
Hughes STX
Greenbelt, Maryland**

ABSTRACT

NASA's Satellite Laser Ranging Network was originally developed during the 1970s to track satellites carrying corner cube reflectors. Today eight NASA systems, achieving millimeter ranging precision, are part of a global network of more than 40 stations that track 17 international satellites. To meet the tracking demands of a steadily growing satellite constellation within existing resources, NASA is embarking on a major automation program. While manpower on the current systems will be reduced to a single operator, the fully automated SLR2000 system is being designed to operate for months without human intervention. Because SLR2000 must be eyesafe and operate in daylight, tracking is often performed in a low probability of detection and high noise environment. The goal is to automatically select the satellite, setup the tracking and ranging hardware, verify acquisition, and close the tracking loop to optimize data yield. To accomplish the autotracking tasks, we are investigating (1) improved satellite force models, (2) more frequent updates of orbital ephemerides, (3) lunar laser ranging data processing techniques to distinguish satellite returns from noise, and (4) angular detection and search techniques to acquire the satellite. A Monte Carlo simulator has been developed to allow optimization of the autotracking algorithms by modeling the relevant system errors and then checking performance against system truth. A combination of simulator and preliminary field results will be presented.

Keywords: satellite laser ranging, autotracking, acquisition, correlation detection.

2. INTRODUCTION

NASA, in cooperation with a large number of international partners, has been operating an international network of manned, centimeter accuracy satellite laser ranging (SLR) systems for over 25 years.¹ The network supports a number of scientific and engineering investigations in the fields of geodynamics, Earth gravity, oceanography, lunar physics, relativity, time transfer, and fundamental physics². In 1996 alone, the number of satellites tracked by laser will increase by 33%, i.e. from 17 to 24. This rapidly increasing workload, combined with falling government scientific budgets worldwide, has spurred development of the "SLR2000" system.

SLR2000 is a system concept for an autonomous, unmanned satellite laser ranging station with a single shot range precision of one centimeter or better. The goal of the program is to provide 24 hour tracking coverage and to reduce both capitalization and operating and maintenance costs by an order of magnitude relative to current outlays. The dominant cost driver in present systems is the onsite manpower required to operate the system, to service and maintain the complex subsystems (most notably the laser), and to ensure that the transmitted laser beam is not a hazard to onsite personnel or overflying aircraft. The SLR2000 system consists of an optical head mounted to a concrete pier which in turn contains a single rack of electronic equipment. The system communicates via Internet for the purposes of obtaining updated satellite schedules and orbits and transmitting range and ancillary data and general housekeeping information.

To keep the cost of the tracking telescope and mount subsystems within reasonable bounds (~\$100K), the SLR2000 telescope aperture is being constrained to a diameter of roughly 30 cm, which is comparable in size to present transportable SLR systems. Single pulse energy is maximized, within eye hazard constraints, by filling the available receive aperture with the transmit beam. Our baseline design assumes use of the 532 nm doubled Nd:YAG wavelength with Single Photoelectron Avalanche Detection (SPAD), but final wavelength selection will depend on the success of programs, external to NASA, in developing a high speed, high quantum efficiency infrared detector.

To counteract the negative effects of a roughly three order of magnitude reduction in laser energy relative to present systems, SLR2000 must operate at kilohertz pulse repetition rates with a three times narrower beam divergence (on the order of 10 arcseconds between $1/e^2$ intensity points) in order to achieve a minimum 100 range measurements within a two minute LAGEOS satellite normal point bin. Such rates and energies can be achieved simultaneously with 100 picosecond pulsewidths by relatively simple diode pumped, Q-switched microlasers and passive multipass amplifiers, thereby eliminating the need for the unreliable and short-lived flashlamps and associated high voltage power supplies, complex switching and modulation electronics, and the long, thermally stable resonators characteristic of modelocked lasers. The microlaser packages are sufficiently lightweight and compact that they can be mounted to the same structure as the telescope, eliminating the need for multimirror Coude systems and vastly improving alignment stability. Beam divergence can be adapted to the satellite being tracked through the use of zoom optics.

To handle the higher repetition rates, event timers similar to those used in lunar laser ranging (LLR) will displace single stop time interval counters in present systems. Station epoch time will be maintained to better than 100 nsec with respect to USNO time by a GPS-steered oscillator. More effective spectral, spatial, and temporal filtering will be required to maintain desirable signal to noise ratios during daylight ranging.

Acquiring and tracking satellites with this extremely low light level system will involve realtime signal detection processing. Current SLR systems rely on the operator to acquire the satellite and compute whatever biases are needed for tracking. SLR2000 must be able to automatically determine signal from noise, and follow the signal by modifying the predictions in realtime. To do this, the system will utilize the information in the "range window" which gives the differences between the commanded and measured ranges shot by shot. Since the error in the measured range is small (less than 70psec), it can be taken to be exact. The data in the range window can then be analyzed using data processing techniques such as Poisson filtering (adapted from LLR) and correlation analysis (discussed later in this paper) to differentiate between signal and noise. Once the signal is found, the predictions can be corrected to center and maintain the ranging returns in the range window and narrow the window itself. To reduce the time spent in acquisition and to increase the number of acquisition successes, we are also working on improving the predictions, by improving the satellite force models used to produce the data, and also by increasing the frequency of updates.

This paper discusses our preliminary development work in determining the SLR2000 system characteristics and acquisition requirements, in developing techniques for differentiating signal and noise, and in automating the acquisition and tracking of satellites. Our work involved the development of a Monte Carlo satellite laser ranging system simulator, whose design, development, and use in testing autotracking algorithms is also presented.

3. ORBITAL PREDICTIONS

The satellite targets for SLR2000 follow a variety of orbits, each of which is determined by fitting tracking data to continuous arcs of several days in length, using a weighted least squares batch data reduction scheme, such as in the NASA developed orbital program, GEODYN. The main limitation to accurately defining and predicting the orbit is error in the dynamic force model. The effect of this error grows in time and so the choice of arc length requires a compromise between definitive orbit accuracy, within the data arc, and predictive capability, for acquisition in the future. Short arcs allow us to define the orbit well, but do not sample the long period model error terms which are important for prediction. Sequential estimators based on Kalman theory, which can also be implemented as modifications to a batch process, can improve definitive orbit accuracy and short-term predictions. However, unless the statistical behavior of the system is well known, sequential methods cannot match the longer term prediction capability of batch methods if they are based on a comprehensive orbit model. The optimum definitive arc length depends on the modeling capability for the particular satellite target, and for well-behaved geodetic satellites, such as LAGEOS, arcs of several months can be fitted to a few centimeters error in the range observations from a large network. These orbits can be used for accurate prediction over several months, with very little error build-up. The largest prediction error is usually along the orbit track, and can be compensated by a timing term, which can be monitored by the network as each station acquires.

The critical modeling factors for orbit determination depend mainly on satellite altitude, and these are listed in Table 1 for a number of different types of retro-reflector-carrying satellites. Spacecraft in lower altitude orbits are strongly affected by atmospheric drag, which is driven by solar flux conditions. In order to model this drag force, the satellite's area to mass ratio should be well

determined, and timely solar flux information must be available, although its behavior is difficult to predict. In general, the lower satellites such as ERS and Starlette are maintained in relatively short arcs of a few days in length, and their prediction accuracy is short-lived. Attitude modeling is also required for non-geodetic satellites such as ERS and Topex, to allow for their orientation relative to the center of mass of the spacecraft, as well as to adequately compute the area exposed to atmospheric drag and solar radiation pressure.

The simple shape of passive retroreflector-only geodetic satellites such as Starlette, Ajisai, LAGEOS and ETALON eases the orbit determination and prediction task. For these targets, the geopotential must be modeled to a resolution which is finer for the lower satellites and must also include orbit-dependent resonance terms. The size of the geopotential force model can be limited to degree and order 12 for high satellites such as LAGEOS and ETALON, but should have 20 by 20 dimensions to adequately model the motion of satellites at Starlette's altitude. The main limitation to orbit determination accuracy for GPS targets is in the solar radiation model, and the description of these vehicles' orbits requires a complex parameterization of the solar pressure forces, as the orbit accuracy depends strongly on eclipse conditions. Much smaller solar radiation and re-radiation forces on LAGEOS and ETALON must be modeled to maintain precise orbit determination for these satellites over long time intervals.

The movement of the station position on the Earth must also be adequately represented if we require an accurate orbit. Polar motion, the movement of the Earth's axis, can be taken from standard sources, or estimated directly from the SLR observations. The

Table 1: Expected SLR2000 Prediction Errors

Satellite	Altitude (km)	Timebias (msec)	Angle Error (urad)	Range Error (nsec)
GPS	20000	100	3.0	200
ETALON	19115	2	0.5	5
LAGEOS	5912	2	0.8	30
AJISAI	1476	10	2.0	40
TOPEX	1337	10	2.0	50
STARLETTE	806	10	4.0	60
ERS-1	783	10	8.0	60

rotational position of the Earth must however be derived from external sources, as the satellite orbit defines a non-inertial system in which station longitude, Universal time, and the right ascension of the node of the orbit cannot be separated. The positions of the stations in a geocentric system can quickly be determined to a few centimeters, although preliminary surveys based on GPS would provide positions adequate for beam pointing.

With the best force models and a modest quantity of ranging data on which to base the prediction, accurate acquisition can be maintained for periods of several days or even months by applying simple along-track error compensation. Complicated or sparsely tracked vehicles present a challenge to timely and accurate look-angle predictions for placing the target within the station's beam, and range predictions for placing the target within the range gate. Search mechanisms have been developed to improve acquisition speed, but as communication become cheaper and computers more powerful, the acquisition process can be simplified by computing the orbits more often, so that errors have less time to build up. Some of the computer power for this new procedure can reside within the instrument, which already has a capable machine for the real-time tracking task, and so each station can share the burden with

a central facility. Testing of more frequently updated predicts is currently taking place in our existing SLR Network. The predicts are produced automatically on a daily basis at a central facility and are electronically downloaded by the stations. Table 1 shows the expected errors in the daily predicts for SLR satellites with various altitudes and characteristics. The timebias is the dominant error source in the predicts, and manifests itself in both angular and range error. The errors in Table 1 were estimated by comparing the predicted data against orbits generated from actual tracking data. Figure 1 plots the errors over the course of a pass for a 75 degree maximum elevation STARLETTE pass. These daily predicts have much smaller errors in both range and angle than the existing operational predicts which can have range errors of a microsecond and hundreds of microradians of angular error due to the uncertainty in the time and crosstrack coordinates. These new predicts are, for many of the satellites, capable of placing the laser beam directly on the satellite without any adjustment, making the system errors (due to unmodeled or time varying misalignments) the dominant error source in acquisition. Results of testing at existing SLR stations, where the laser divergence is larger than most of the systematic errors, show that systems can acquire the satellites using these new predicts immediately upon the start of tracking.

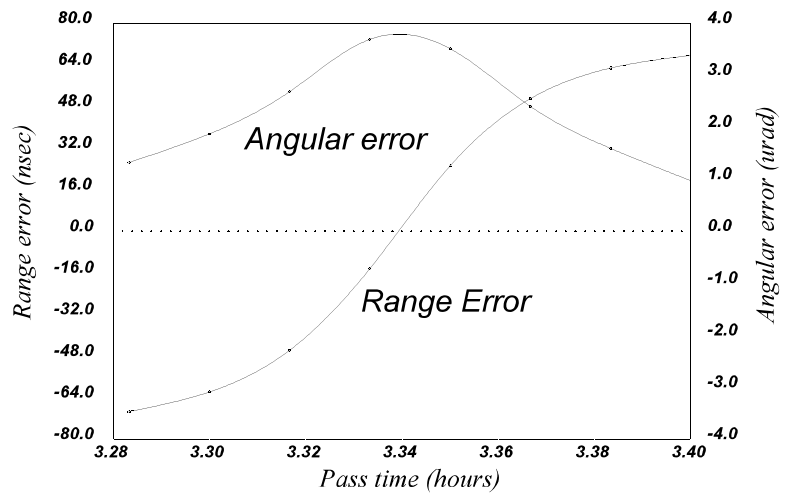


Figure 1: Example of STARLETTE prediction errors

4. ACQUISITION REQUIREMENTS

All target satellites must be tracked by SLR2000 in a totally autonomous fashion. Key orbit characteristics for some typical SLR target satellites are provided in Table 2. We assume in presenting the optical radar cross-section data that the three basic functions - acquisition, tracking, and ranging - will be accomplished using some combination of the fundamental and second harmonic wavelengths of the Nd:YAG laser at 1064 and 532 nm. Our initial uncertainties in angular pointing, time, and range are based on hardware characteristics, past experience, and analyses of the type presented in the last section.

Table 2: Typical Target Satellites* Characteristics and Acquisition Requirements^{3,4}

	Starlette	LAGEOS	GPS
Altitude (km)	960	5,900	~ 20,000
Period (Hr/Min/Sec)	1/43/55.8	3/45/26.5	11/49/4.14
Velocity (km/second)	7.39	5.7	3.894
Maximum Time-in-View, 20° to 20° (Minutes)	8.805	51	239.86
Maximum Slew Rate (milliradians/second)	7.7 @ zenith	0.967 @ zenith	0.195 @ zenith
Initial Acquisition Elevation Angle (Degrees)	< 20°	< 20°	~30°
Cross-Section: 5320 nm / 1064 nm (10 ⁶ meters ²)	0.65 / 0.52	7 / 5.7	18 / 14.4
Initial System Pointing Uncertainty (μ-radians)	± 72.7	± 72.7	± 72.7
Initial Time Uncertainty (msec)	± 10	± 2	± 100
Derived Acquisition Angular Uncertainties (μ-radians)	± 80 @ 20° El ± 120 @ 90° El	± 80 @ all El	± 80 @ all El
Initial Range Uncertainty (nsec)	± 100	± 100	± 200
Maximum Initial Rate of Change of Range Rate (nsec/sec ²)	~ 300	~ 10	< 1
Time to Acquire (seconds)	< 10*s	up to 120	up to 300
Probability of Acquisition	~ 90%	~ 90%	~90%
Eye-Safety	At aperture	At aperture	At aperture

5. EYE SAFETY

To keep the cost of the tracking telescope and mount subsystems within reasonable bounds, the SLR2000 telescope aperture is presently constrained to about 30 cm, which is comparable in size to present NASA transportable systems. Furthermore, it was decided early in our deliberations that eyesafe beams are to be preferred over active aircraft radars in ensuring eye safety. Taking this approach has several important advantages. From an engineering and economic standpoint, the passive eyesafe approach is absolutely failsafe and eliminates the need for an additional large and expensive aircraft radar subsystem. Furthermore, from a political and legal standpoint, it should be easier to obtain approval from local regulatory agencies, such as the Federal Aviation Administration (FAA) in the United States for such a system to operate in an unattended mode. The principal disadvantage is that combining the eyesafe requirement with the small aperture results in a maximum single pulse energy which is significantly less than a millijoule at the visible and near infrared wavelengths commonly used in SLR. As we shall see shortly when we discuss probability of detection, SLR2000 must operate at kilohertz pulse repetition rates with a narrower beam divergence on the order of 10 arcseconds (between $1/e^2$ intensity points) in order to counteract the negative effect of a roughly three order of magnitude reduction in laser energy relative to present systems and to achieve a minimum 100 range measurements within a two minute LAGEOS normal point bin. However, such rates and energies can be easily achieved simultaneously with 100 picosecond pulsewidths by a relatively simple Q-switched microlaser followed by a single multipass amplifier. It is demonstrated elsewhere that a Nd:YAG microlaser operates most efficiently at roughly a 2 KHz rate when pumped by a CW diode.⁵ These microlaser packages are sufficiently lightweight and compact that they can be mounted to the same structure as the telescope, eliminating the need for multimirror Coude systems and vastly improving long term alignment stability.

Clearly, single pulse energy is maximized, within the eye hazard constraints, by filling the available aperture with the transmit beam. In calculating the eyesafe energy at a particular wavelength according to U.S. ANSI standards,⁶ one must take into account cumulative multiple pulse effects on the human retina according to the equation

$$E_{\max} = MPE(PR F * T)^{-1/4} A$$

where E_{\max} is the eyesafe energy, MPE is the maximum permissible exposure ($5 \times 10^{-7} \text{ J/cm}^2$ @ 532 nm and $5 \times 10^{-6} \text{ J/cm}^2$ @ 1064 nm), PRF is the pulse repetition frequency, T is the exposure time in seconds, and A is the area of the telescope aperture. For visible wavelengths, readily seen by the observer, a reaction or integration time of 0.25 seconds must be assumed. For infrared wavelengths, invisible to the observer, the ANSI standards require longer integration times on the order of ten seconds. Assuming a repetition rate of 2 kHz and an aperture area $A = 0.07 \text{ m}^2$, the maximum allowable transmitted energy per pulse is 297 microjoules for the fundamental (1064 nm) and about 75 microjoules for the frequency-doubled (532 nm) wavelengths of Nd:YAG respectively.

Energy per Pulse (uJ)	
532nm	1064nm
75	0
70	47
60	147
50	247
40	347
30	447
20	547
10	647
5	697
0	297

We hypothesize that, if both wavelengths are present simultaneously, the pulse exposure time can be reduced to 0.25 seconds for both wavelengths resulting in an expression for the total eyesafe energy given by

$$E_{\text{tot}} = E_{532} + 0.1E_{1064} = 75\mu\text{J}$$

Table 3: Simultaneously Eye-safe Energies/Pulse

Table 3 shows the trade-off between green and infrared energy provided by the latter equation for 2 kHz PRF and 30 cm aperture diameter telescope. Subsequent analyses performed in this paper assume 30 uJ of green laser energy and 447 uJ of infrared.

In the authors' opinion, the use of so-called "eyesafe" wavelengths longer than about 1.4 microns does not, at least at the present time, offer any real advantages to SLR2000. These wavelength regions suffer from relatively inefficient, low gain, and technologically immature laser materials and exotic detector materials typically characterized by relatively low quantum efficiency and high internal noise. Furthermore, going to longer wavelengths to take advantage of the higher eyesafe pulse energies reintroduces many of the undesirable features of high energy laser systems which are largely eliminated by the use of the low energy, diode-pumped microlaser. For example, high energy lasers must be pumped either by flashlamps (with their accompanying large high voltage power supplies and cooling systems) or by rather expensive high power laser diode arrays. Furthermore, these larger lasers are more likely to damage optics and cannot be directly mounted to a small telescope which then requires the use of

a more complex Coude or similar multimirror system, further increasing cost and endangering the long term reliability and alignment stability in an unattended mode.

6. OPTICAL RADAR LINK EQUATION

The mean number of signal photoelectrons seen by the detector is given by the radar link equation¹

$$n_{pe}^s = \eta \left(\frac{E_p}{h\nu} \right) \gamma_t \tau_a \tau_c \left(\frac{\sigma}{\pi (\theta_t \gamma_{trb})^2 R^2} \right) \tau_c \tau_a \gamma_r \left(\frac{A_r}{\pi R^2} \right) G$$

The definitions of the parameters used in the above equation, the values used for analysis, and the minimum elevation angles for three satellites, are given in Table 4. Figure 2 presents daylight 532 nm results for the three satellites, for all elevation angles.

Table 4: Parameters for Satellite Signal Level Estimation

Parameter	Symbol	Value for 532 nm	Value for 1064 nm
Quantum Efficiency	O	0.40	0.20
Energy /pulse at aperture(μJ)	E _p (_t)	30	447
Photon Energy (J)	h<	3.73 (10 ⁻¹⁹)	1.87 (10 ⁻¹⁹)
One way path transmission	J _a J _c	0.75 @ 20° elevation 0.12 @ 20° elevation	0.8 @ 20° elevation 0.15 @ 20° elevation
Optical Cross-section (m ²)	F	0.65(10 ⁶) for STARLETTE 7 (10 ⁶) for LAGEOS 20 (10 ⁶) for GPS	0.52 (10 ⁶) STARLETTE 5.7 (10 ⁶) LAGEOS, 14.4 (10 ⁶) GPS
Slant Range (Km): Starlette LAGEOS GPS	R	2052 @ 20° elevation 8532 @ 20° elevation 23503 @ 30° elevation	same as for 532nm
Receiver Optics Transmission	(_r	0.12 (day) 0.50 (night)	0.12 (day) 0.50 (night)
Receiver Area (m ²)	A _r	0.07 for 30 cm diam.	0.07 for 30 cm diam.
Turbulence Parameter	(_{trb}	1.5	1.25
Aperture Fitting Parameter	G	0.5	0.5
Transmitter half-angle beamwidth (μrad)	Z _t	20	20
Mean signal pe's per pulse Starlette (20°) LAGEOS (20°) GPS (30°)	n _{pe} ^s	cirrus / clear 0.0028 / 0.194 0.000078 / 0.0054 0.00015 / 0.0104	cirrus / clear 0.136 / 6.06 0.00483 / 0.215 0.0025 / 0.0159

The above quantum efficiency is available in the green either from European developers of Single Pulse Avalanche Detectors (SPADs), or in a more conventional form as Model 280 Intensified Photo-diodes from Intevac ATD. The 1064 nm quantum efficiency is available in a photon counting developmental device, the TE-IPD, currently being developed by EOO, Inc. and Intevac ATD under a NASA/GSFC SBIR.

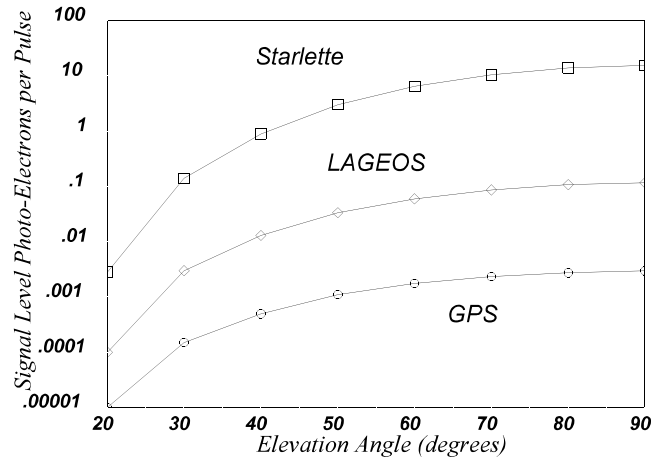


Figure 2: Mean single pulse photo-electron levels for a 532nm beam under daylight cirrus conditions and using the parameters in Table 4

7. OPTICAL BACKGROUND NOISE

The governing equation is $n_{pe}^b = \left(\frac{\eta}{h\nu} \right) N_v(\lambda) B_{opt} \Omega_r A_r \gamma_r T$ where $N_v(\lambda)$ is the background spectral radiance in

watts/meter²-ster-Å, B_{opt} is the optical filter bandpass in Å, $S_r = B_r^2$ is the solid angle field-of-view in steradians, and 2_r is the half angle of the receiver field-of-view in radians. This equation is evaluated in Table 5 for both green and infrared. The night-time values are negligible, but the daytime values are comparable to the signal levels.

Table 5: Background photo-electrons per range gate, 532 and 1064 nm, using parameters from Table 4, with $B_{opt}=1.0$ D and $S_r=9.6(10^{-10})$ steradians.

Condition	532 nm Background Spectral Radiance ⁴ : $N_v(\lambda)$ (watts/meter ² -srad-Å)	532 nm-generated photo-electrons per 1 usec range-gate: n_{pe}^b	1064 nm Background Spectral Radiance ⁴ : $N_v(\lambda)$ (watts/meter ² -ster-Å)	1064 nm-generated photoelectrons per 1 usec range-gate: n_{pe}^b
Night: Clear	$1.46 (10^{-8})$	0.00000014	$7.3 (10^{-9})$	0.000000016
Day: Clear	$1.46 (10^{-3})$	0.014	$7.3 (10^{-4})$	0.0016

8. DETECTOR DARK CURRENT NOISE

Even in the absence of optical background noise, some detectors generate a substantial dark count rate which will compete with

the valid signal pulses. The governing equation is given by $n_{pe}^{dc} = \left(\frac{I_d}{e} \right) T \frac{\pi}{4} D_d^2$ for single pixel devices, while for multi-

pixel detectors or receivers the expression is
$$n_{pe}^{dc} = \left(\frac{I_{dc}^{pix}}{e} \right) T$$
 where I_d is the dark current density at the cathode in

amps/cm², e is the electron charge (1.6×10^{-19} coulombs), D_d is the diameter of the photocathode (cm), i_{dc}^{pix} is the dark current in amperes per pixel or array element at the cathode equal to i_{dc}/N_{pix} and where i_{dc} is the total cathode dark current and N_{pix} = number of pixels in the field of view / detector array.

For a single pixel green receiver, assuming a typical dark current density of 10^{-15} amps/cm² and a cathode diameter of 1.2 cm, the number of dark counts in a 1 usec range gate is 0.007. For a 16 pixel 1064 nm TE detector, and for a total cathode dark current of 0.1 picoamps, the number of dark counts in a 1 usec range gate = 0.039 per pixel. As can be seen from Figure 2, these levels are commensurate with the signal levels for the higher satellites. Autotracking will, therefore, require the development of analysis techniques to extract the signal from the noise.

9. TARGET ACQUISITION

Acquiring the satellite consists of determining if the system is hitting the satellite, estimating how far off the range and angles are, and then making use of that information to optimize the pointing and ranging control. Also required in the acquisition scenario is

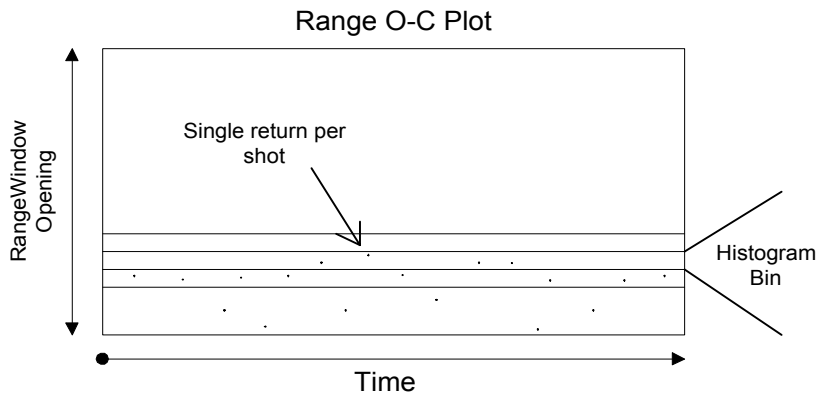


Figure 3: Returns in the Range Window

the ability to search for the satellite if no signal is found, and to be confident that the algorithm being used will seldom fail to find the signal or mistake noise for satellite signal. As can be seen from the above discussion, for SLR2000 all acquisition must be accomplished in an environment where the expected mean per pulse signal returns are in general quite small, even with a relatively narrow ± 20 rad beamwidth, and where the daylight noise rates are comparable to the mean signal levels, even assuming reasonable range gates of 100 nsec to 1 sec.

The range return is the SLR's most accurate measurement (1cm shot to shot) and is therefore the best information to make use of in the acquisition process. Range returns are analyzed in the form of observed minus calculated (O-C) graphs where the range returns minus the predicted ranges (called range deltas) are plotted on a shot by shot basis in the range window as shown in Figure 3. When the prediction biases are held constant, the range deltas form a straight line for a period of up to many seconds. The slope of this line is a function of the error in the dependent variable, time (called timebias). With the advances in the accuracy of the predictions, this error has become small. This gives the range delta plots a very small slope, and causes the range deltas to change very little in vertical positioning over the course of a few seconds.

We are investigating two methods for distinguishing signal from noise in the range window. Both generate a histogram from O-C data by binning the range deltas over a period of time. Both rely upon a small slope in the range delta data to ensure that most of the signal will fall within a single histogram bin. Lower expected return rates, higher range rates, and larger errors in the timebias all require an increase in the histogram bin size. The optimum bin size is just large enough to ensure that the signal remains in a single bin, since the larger the bin, the higher the noise count, and the higher the probability of false acquisition. The range-rate and the information in Table 1 is known, but other parameters (such as atmospheric transmission) are unknown and must be accounted for conservatively in any algorithm.

9.1 Acquisition Probability

The Poisson Filtering Algorithm was developed for Lunar Laser Ranging in the late 1960s⁷ and was ported to Satellite Laser Ranging analysis in the late 1980s⁸ to remove noise in the non-realtime post processing and analysis of the data. In current SLR data, the signal to noise ratio is often extremely high whereas, in the SLR2000 system, the signal will often be dominated by the

noise, as is true in the lunar case. Unlike the lunar case, however, the nonzero O-C slope and possible nonzero range bias of the data adds an extra challenge in the algorithm development. The algorithm uses the number of returns over a period of time, called a Frame, to estimate the noise rate. The noise is assumed to be Poisson. A histogram of the range window is generated as shown in Figure 3, and the noise rate is divided by the number of bins to find a noise rate per bin. Assuming a Poisson distribution for the number of noise returns per bin, the algorithm then determines a noise count which has less than a 50% probability. Any bin which has more returns in it than this count is assumed to be signal. If no bin has more returns than this number, the process can be extended and the histogram continues to fill until either the signal is found, or the period of time becomes too long.

The Correlation Detection Technique, which members of our team developed, also produces a histogram of the range deltas. In this process, however, multiple Frames are examined to see if any bin is correlated in at least two of the Frames. Here correlation is defined as having three or more points in the same bin. For an algorithm to be viable the probability that the signal will be correctly identified must be greater than 90% and the probability of incorrectly identifying noise as signal must be less than 10%. The probability that three or more signal photo-electrons are detected by correlation identification is given by

$$P_K(\geq 3) = 1 - \left(1 + N_{pe}^S + \frac{(N_{pe}^S)^2}{2!} \right) e^{-N_{pe}^S}$$

where:

n_{pe}^S = mean # signal photoelectrons per return

N_{pe}^S = mean # of signal photoelectrons after K returns

K = # of range returns accumulated before a decision is made (called a Frame).

We can see from Figure 4 that in order to have greater than 90% probability of successful correlation detection the mean value of signal returns must be 6 or more. From the expected signal levels in Figure 2, this means that for LAGEOS (daylight cirrus at 30 degrees elevation) the Frame must be three-quarters of a second, for STARLETTE (daylight cirrus at 20 degrees elevation) a quarter of a second is sufficient, and for GPS (daylight cirrus at 30 degrees elevation) the Frame will have to be 20 seconds long. Tracking GPS during the night, however, allows a broader band spectral filter to be used, which increases the system transmission. Here the expected return for GPS is four times greater, improving the Frame size to 5 seconds. The uncertainty in the timebias (from Table 1), along with the satellite range rate error and the Frame times determine the histogram bin size for each satellite. Table 6 lists the bin sizes required for each.

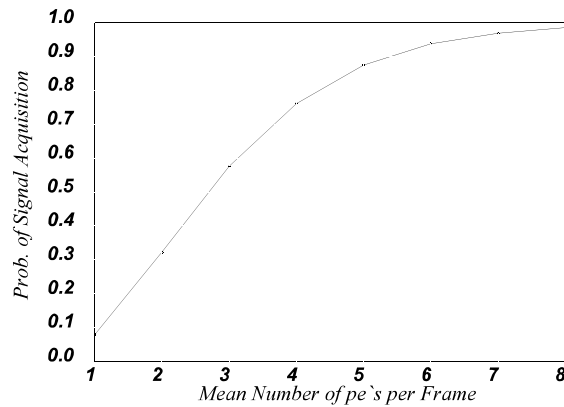


Figure 4: $P_K(\geq 3)$

Table 6: Correlation Detection Histogram Bin Size Requirements (532nm)

Satellite	Prediction timebias (seconds)	Rate of change of range rate (nsec/sec ²)	Time (seconds) for 5 Frames	Bin size (nsec)
Starlette (day)	0.010	300.	1.25	3.75
LAGEOS (day)	0.002	10.0	3.75	< 0.50
GPS (day)	0.100	0.4	100.0	4.0
GPS (night)	0.100	0.4	25.00	1.0

9.2 False Acquisition

The problem of false correlations, caused by noise photoelectrons generated by the optical background or the cathode dark current, is equally as important as a successful correct identification of signal. The governing equation is:

$$P_{FalseAlarm} = 1 - \left[e^{-\frac{m}{n_{bin}}} \sum_{x=0}^{k-1} \frac{\left(\frac{m}{n_{bin}}\right)^x}{x!} \right]^{n_{bin}}$$

where
 m = the mean number of noise photoelectrons collected during the decision time (ie the Frame)
 k = the correlation number (k=3 here)
 n_{bin} = number of histogram bins.

This equation applies during both acquisition and ranging, but false correlation is more of an issue during acquisition because the number of noise photoelectrons may be far greater per bin due to the larger bin size required. Using the numbers given in Table 6 required for successful signal identification and the expected noise levels during a clear day for optical background at 532nm (1.46x10⁻³ watts/meter²-srad-D) and detector dark current (1x10⁻¹⁵ amps/cm²), we see in Table 7 that all three satellites can be successfully acquired and tracked at 532nm using Correlation Detection except for GPS during the daylight. More work is required to determine if an algorithm can be developed that can acquire a GPS daylight pass at 532nm. The possibility of using the infrared for acquisition instead of the green is also being investigated, and the next section presents some of our analysis of acquisition using the infrared. Simulator tests using the Table 7 values are shown at the end of this paper.

Table 7: Probability of False Correlation (532nm) for a 1: sec Range Gate

Satellite	Noise (pes/gate)	Bin Size (nsec)	Frame Time (# shots)	Average noise in Frame per bin (m/n _{bin})	# Bins (n _{bin})	Probability of False Correlation
Starlette(day)	0.02	3.75	500	0.013	266	negligible
LAGEOS(day)	0.02	0.50	1500	0.020	2000	0.3%
GPS (day)	0.02	4.00	40,000	1.136	250	100%
GPS(night)	0.007	1.00	10,000	0.071	1000	5.5%

9.3 Angular Aids to Acquisition

Finally, the system must be able to put the laser beam on the satellite in order to acquire and track. We have been examining the use of the 1064nm beam for angular corrections. From Table 2, the initial angular uncertainty during acquisition is typically ±80: rad. Since a typical cone of uncertainty will encompass about 16 beamwidths, target acquisition will require the implementation of one of the acquisition approaches described in Table 8.

Table 8: Appropriate Acquisition Approaches

Transmitter Beam	Receiver/Detector	Comment
Full uncertainty beam	Full uncertainty receiver FOV	Minimum SNR; Requires zoom for localization
Full uncertainty beam	Multiple pixel	Better SNR; multiple parallel processing, zoom transmitter
Small beam, << uncertainty	Small (single pixel)	Best SNR, minimal parallel processing, scanning required
Intermediate Size beam	Intermediate number of pixels	Balance for optimization, some combination of parallel processing, zooming, and scanning will be required

We must treat this acquisition process like a photon counting optical radar, in which case only 1064 nm photon counting detectors are useful -- the Geiger Mode APDs (GM-APDs or SPAD) and the emerging TE device mentioned earlier.

The same method of Correlation Detection described for 532nm will be used in the identification of the signal for each of the 1064nm detectors. When analysis of acquisition was examined for high satellites (such as LAGEOS and GPS) with the large (80

: radian) beams and the 16 pixel detectors, it was found that the Probability of False Acquisition was 100%. Consequently, we considered a small spot transmitter (20 : radians) and a 2 x 2 pixel receiver. This means that 16 spots must be scanned in order to cover the same uncertainty area as for the fully flooded technique. The signal beam is, however, sixteen times smaller, so the signal photo-electron rate is 16 times greater which means that the same probability of signal acquisition can occur 16 times faster, the frame length can be 16 times smaller, and the number of noise photo-electrons per 20 : radian field of view would in turn be 16 times smaller.

Analysis using Correlation Detection for a 200 nsec range gate with a noise rate of 63.3 pe/sec in the gate gives 0.01 for a probability of false acquisition. This result shows substantial design freedom. The single frame dwell time required for this acquisition is 0.4 seconds, so the 16 spots would be actively viewed for 6.4 seconds. Since the acquisition requirement is 120 seconds, there is more than enough time to accelerate, move, and settle between the spots.

For the low satellites (such as Starlette) we considered the full flood beam again, and the False Acquisition Probabilities varied from 23% to 53%, which we consider to be very marginal performance. On the other hand, using the 20 : radian beam and the 2 x 2 detector, the Probability of False Acquisition was ≈ 0.01 . We also, therefore, considered an intermediate case, with a 40 : radian transmit beamwidth and the 2 x 2 detector, which gave a Probability of False Acquisition of 3%. This is good performance which allows for modifications to the design parameters, and requires a maximum dwell time of $4 \times 0.125 = 0.5$ seconds, with four spots to be addressed by the scanner over the allowable 10 seconds. Since it only requires processing of 4 channels of information, this is our design choice.

A summary of the 1064nm acquisition hardware and performance parameters (for the lowest elevation angles and worst case path transmission) are given in the following two tables.

Table 9: 1064 nm Acquisition Baseline Hardware Parameters

Transmitter	Receiver
Wavelength: 1064 nm	Filter Bandpass: 1 Å
Energy Per Pulse at Aperture: 447 µjoules	Detector Quantum Efficiency: 20%
Average Pulse Repetition Frequency: 2 kHz	Detector Mode: Photon Counting
Average Power at the Aperture: 0.894 Watts	Cathode Dark Current: 10^{-13} amps
Pulsewidth: < 500 picoseconds (nominal)	Resolution: < 1 nanosecond
Transmitter Aperture: 30 cm diameter	Receiver Aperture: 30 cm diameter
Optics Transmission: Implicit in energy and power levels at the transmitter aperture	Optics Transmission: 12%, receiver aperture to detector cathode
Transmitter Beamwidth: Selectable, depending on satellite target	Receiver Field-of-View: Selectable, depending on satellite target.
Green output During Acquisition: 30 µjoules per pulse, 2 kHz, at the transmitter aperture	Pixilated Field of View / Multiple Pixels per Detector or multiple Detectors

Table 10: Optical beamwidths, Fields-of-View, Acquisition Times, Scanner and Zoom Optics Parameters

	Starlette	LAGEOS	GPS
Transmitter Beam Width (Half-Angle), µradians	40	20	20
Receiver FOV (per pixel) (Half-Angle), µradians	20	10	10
Time to Acquire (per spot), seconds	0.125	0.4	0.4
Initial Angular Uncertainty, µradians	± 80 by ± 80	± 80 by ± 80	± 80 by ± 80
Required Number of "Spots"	~ 4	~ 16	~ 16
Time to Cover the "Spots", seconds	0.50	6.4	6.4
Total Scanner Overhead Time Allowed, seconds	9.50	113.6	293.6
Zoom Optics Range	2:1	1:1	1:1

It is anticipated that tracking will continue after acquisition, during the ranging function, by continued use of the 1064 nm signal and the quadrant detector. We estimate that drift corrections could be provided even at the lowest elevation angles with update rates of 0.2 seconds for Starlette and 6.5 seconds for the higher satellites.

10. SLR2000 SIMULATOR

The SLR simulator was developed to check candidate autotracking algorithms prior to hardware development. Figure 5 shows the overall block design. A main routine provides operator interaction, inputs the required parameters and develops the desired plotting data and statistical information. A separate subroutine computes the “Truth” about the satellite’s position, a “Hardware” subroutine calculates the system response to the satellite tracking and ranging, while the “Field Software” subroutine performs the tasks expected of the onsite computer(s). The simulator can be used to test algorithms for extracting signal from noise, automated acquisition and tracking, and realtime prediction update. The program models the tracking subsystem, the receiver subsystem, the laser, the satellite, the environment, and their associated errors. Only those parts of these subsystems that affect the autotracking are modeled; there is no attempt to make a complete system simulation. The functions/errors modeled in the simulator are shown in Table 11. The models used include those given in this paper along with others from the references.^{1,9} Table 12 lists the parameters used in the simulation test results. For the most part these values match those given in Table 4.

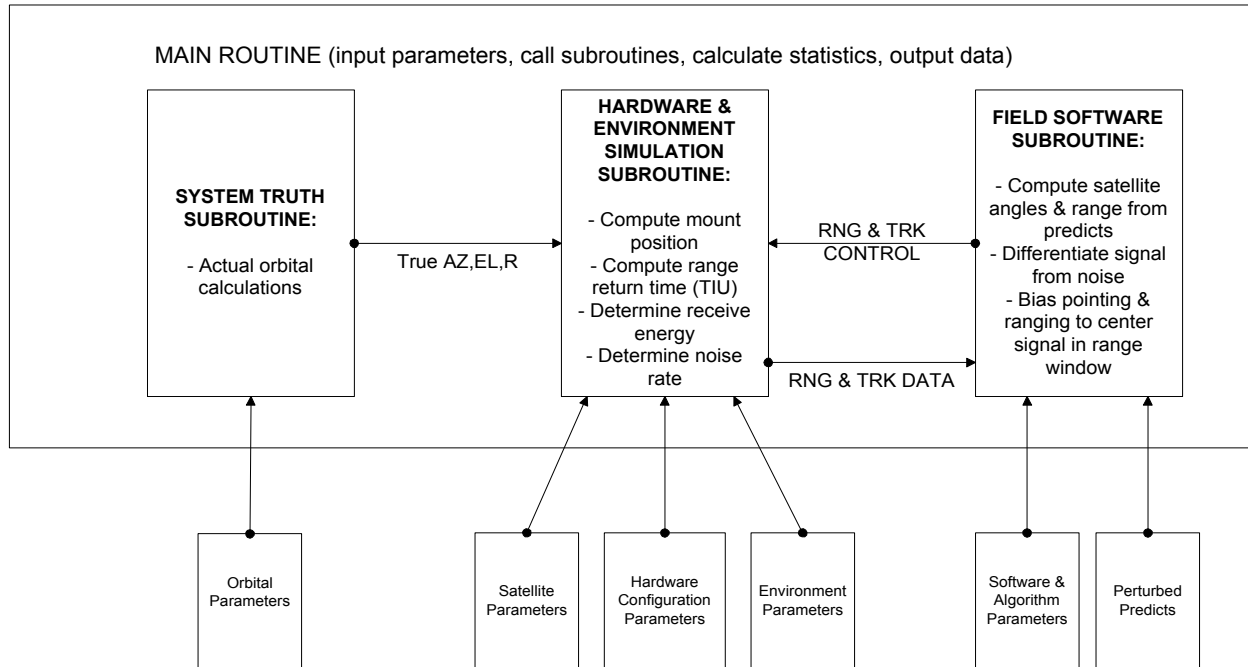


Figure 5: SLR2000 Simulator Design

Both the Poisson Filtering Technique and the Correlation Detection Technique were incorporated as subroutines into the Simulator for extracting signal from noise. Either algorithm can be used, and both have been tested with success. The plots in Figure 6 show simulator test results for acquisition of STARLETTE, LAGEOS and GPS using the Correlation Detection Technique. The plots show all events (noise or signal) in the range window as dots; this would be what the SLR2000 system would see. The squares mark actual returns from the satellite; this information is not available to the SLR2000 system. Initially the predictions contain errors in both time and range. The Field Software collects the data and every Frame runs the Correlation Detection Algorithm to check if there are satellite returns. Once the signal is found, the field software calculates and applies the required time and range biases needed to center the range returns in the window. The field software then closes the range window down to 10 nanosecond and enters tracking mode. The STARLETTE and LAGEOS tests were during daylight but due to the narrow filter used (1.0 D) and relatively narrow range gate (1 : sec) little noise enters the range window. The prediction timebias error for the STARLETTE pass was 10 milliseconds, and the histogram binsize used was 3.75 nanoseconds. The LAGEOS prediction timebias error was 2 milliseconds, and the histogram binsize used was 0.5 nanosecond. The short Frame time, coupled with the small timebias, gives the signal a nearly zero slope in the range window and allows both algorithms to work successfully.

The signal level from the GPS satellite is extremely low, due to a relatively small reflector area for its high altitude,¹⁰ and is not representative of other satellites at this altitude such as Etalon and GLONASS. Because this pass was at night, the system was able to use the 3 D filter (ensuring a higher signal rate due to this filter’s higher transmission). The Frame used was 5 seconds, and the algorithm took the minimum 10 seconds to find the satellite. The prediction timebias error for this pass was 100 milliseconds and, due to the small GPS range rate, the algorithm was still able to use a histogram binsize of 1.0 nanosecond. The Poisson Filtering Algorithm yielded similar results for all three cases. Neither algorithm, however, was able to find the GPS signal

in the daylight.

Table 11 Functions/Errors currently modeled in the Simulator	Table 12 Hardware Parameters for SLR2000 Test Runs
<ul style="list-style-type: none"> ● Pointing System <ul style="list-style-type: none"> - Bias of mount system (error in mount model) - Random repeatability error ● Receiver Timing <ul style="list-style-type: none"> - Model receiver (PMT or photon-counting APD) - TIU error modeled as random Gaussian noise - Assume no gating error or start time error - Compute background noise above threshold - System delay bias can be applied ● Receiver Energy <ul style="list-style-type: none"> - Assume fixed transmitter energy - Assume Gaussian pulse - Compute transmitter gain as function of laser divergence - Attenuate with system and atmospheric transmission - Attenuate as function of pointing error - Treat satellite as single cube with given cross-section 	Shot repetition rate.....2000 Hz Wavelength.....532 nanometers Spectral bandwidth.....1.0 (day) / 3.0 (night) Laser divergence.....20 urad (half-angle) Transmit energy.....30 microjoules Mount repeatability.....5 urad (1-sigma) Mount model error.....7.2 urad (1-sigma) System delay.....20 nanoseconds TIU error.....0.02 nanoseconds (1-sigma) Receiver area.....0.071 meters ² Receiver FOV (solid angle).....9.6D-10 steradians System transmission (rcv).....0.12(day) / 0.50(night) Detector quantum efficiency.....0.40 Detector dark current.....1.0D-15 amps Atmospheric transmission.....0.75 (at zenith) Solar irradiance (day).....0.0014 Watts/Ang-ster-m ² GPS lidar cross-section.....20.0D6 meters ² LAGEOS lidar cross-section.....7.0D6 meters ² STARLETTE lidar cross-section.....0.8D6 meters ²

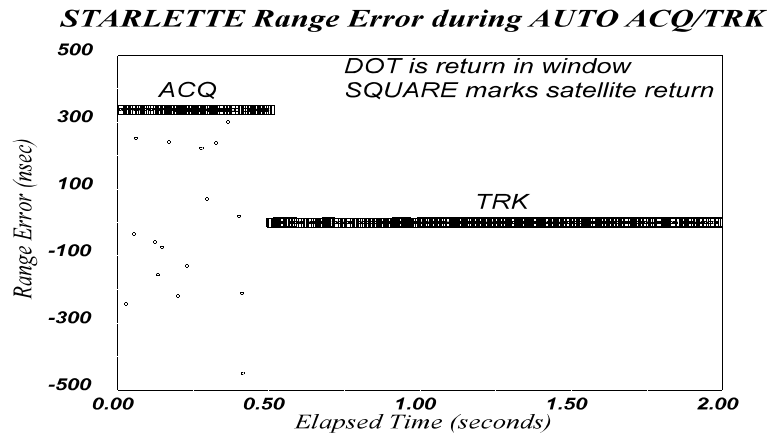
11. CONCLUSION

We have demonstrated that a low energy, high repetition rate, eye-safe satellite laser ranging system can be designed to acquire and track the existing constellation of laser ranging satellites. Whether the high satellites such as GPS can be tracked during the daylight is unclear as yet, and the details of how this system will be automated remains to be determined. Theory and simulation, however, both show that with the emerging technologies available, there will be enough margin between signal and noise to acquire and track all current and planned retro-reflector carrying satellites.

12. REFERENCES

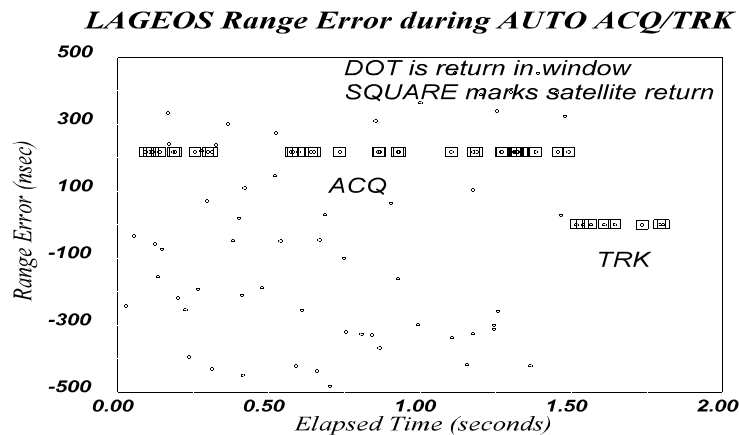
1. Degnan, John J., "Millimeter Accuracy Satellite Laser Ranging: A Review," in Contributions of Space Geodesy to Geodynamics: Technology, D.E.Smith and D.L.Turcotte (Eds), AGU Geodynamics Series, Volume 25, pp 133-162, 1993.
2. Degnan, John J. (Ed.), Satellite Laser Ranging in the 1990's: Report of the 1994 Belmont Workshop, NASA Conference Publication 3283, Nov.1994.
3. Titterton, Paul, and Harold Sweeney, SLR2000 Design and Processing Sensitivity Approach, EOO Report 94-003, December 15, 1994.
4. Titterton, Paul, and Harold Sweeney and Thomas Driscoll, SLR 2000 Analytical Study of 1060 nm Aided Acquisition and Tracking, EOO Report 95-007, November 1, 1995
5. Degnan, John J., and Joseph Dallas, "Q-switched microlasers: A reliable alternative to modelocking," Proceedings of the 9th International Workshop on Laser Ranging Instrumentation, Canberra, Australia, Nov 1994 (to be published).
6. ANSI Z136.1-1993, Section 8.2, Table 5 and the Errata Sheet, 1993.
7. Abbot, Richard I., Peter J. Shelus, et al, "Laser Observations of the Moon: Identification and construction of normal points for 1969-1971," The Astronomical Journal, Vol 78, No.8, October 1973.
8. Ricklefs, R.L., P.J.Shelus, "Poisson Filtering of Laser Ranging Data," Proceedings of the Eighth International Workshop on Laser Ranging Instrumentation, NASA Conference Publication 3214, May 1992.
9. Abshire, James B., Jan F. McGarry, et al, "Laser Altimetry Simulator, Version 3.0," NASA Technical Memorandum 104588, January 1994.
10. Degnan, John J., and Erricos C. Pavlis, "Laser Ranging to GPS satellites with centimeter accuracy," GPS World, pp.62-70, September 1994.

**Figure 6: SLR2000 Simulator Acquisition Testing
(Returns in the Range Window)**



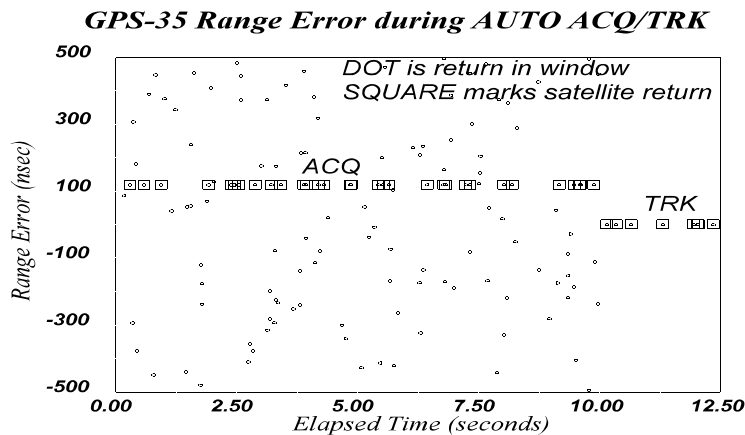
Initial two seconds of a Starlette pass on 41/1996 at 19:18Z (Daylight)

Timebias of predicts = 10 msec
Elevation of satellite at acq = 20 deg



Initial two seconds of a LAGEOS pass on 41/1996 at 18:18Z (Daylight)

Timebias of predicts = 2 msec
Elevation of satellite at acq = 30 deg



Initial twelve and a half seconds of a GPS35 pass on 51/1996 at 03:41Z (Night)

Timebias of predicts = 100 msec
Elevation of satellite at acq = 30 deg